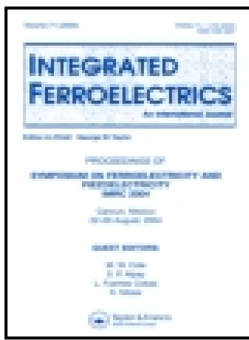

Taylor & Francis
Taylor & Francis Group

Integrated Ferroelectrics

ISSN: 1058-4587 (Print) 1607-8489 (Online) Journal homepage: http://www.tandfonline.com/loi/ginf20

THIN-FILM PIEZOELECTRIC ACTUATORS FOR BIO-INSPIRED MICRO-ROBOTIC APPLICATIONS

KENN OLDHAM , JEFFREY PULSKAMP , RONALD POLCAWICH , PRASHANT RANADE & MADAN DUBEY

To cite this article: KENN OLDHAM , JEFFREY PULSKAMP , RONALD POLCAWICH , PRASHANT RANADE & MADAN DUBEY (2007) THIN-FILM PIEZOELECTRIC ACTUATORS FOR BIO-INSPIRED MICRO-ROBOTIC APPLICATIONS, Integrated Ferroelectrics, 95:1, 54-65, DOI: 10.1080/10584580701756482

To link to this article: http://dx.doi.org/10.1080/10584580701756482

Published online: 20 Sep 2010.

Submit your article to this journal

Article views: 172

View related articles

Citing articles: 12 View citing articles

Full Terms & Conditions of access and use can be found at
http://www.tandfonline.com/action/journalInformation?journalCode=ginf20

Download by: [University of Michigan] **Date:** 13 June 2017, At: 12:44

Integrated Ferroelectrics, 95: 54–65, 2007
Copyright © Taylor & Francis Group, LLC
ISSN 1058-4587 print / 1607-8489 online
DOI: 10.1080/10584580701756482

Taylor & Francis
Taylor & Francis Group

Thin-Film Piezoelectric Actuators for Bio-Inspired Micro-Robotic Applications

Kenn Oldham,[1,*] Jeffrey Pulskamp,[2] Ronald Polcawich,[2] Prashant Ranade,[2] and Madan Dubey[2]

[1]Oak Ridge Associated Universities, Oak Ridge, TN
[2]United States Army Research Laboratory 2800 Powder Mill Road Adelphi, MD 20783

ABSTRACT

Biologically-inspired autonomous micro-robots have a variety of anticipated applications resulting from their unique scale and cooperative potential. To achieve locomotion comparable to biological systems, these micro-robots will require actuators substantially stronger than most existing MEMS actuation technologies. Piezoelectric thin-films can meet these specifications while drawing limited power and contributing little mass to micro-robotic systems. Theoretical actuation requirements for micro-robotic applications show that lead-zirconium-titanate (PZT) thin-film actuators can meet these requirements, including a new thin-film PZT lateral actuator developed by the United States Army Research Laboratory. Experimental results and a comparison to other common lateral actuation technologies are presented.

I. INTRODUCTION

The realization of autonomous micro-robots at the millimeter scale could produce robotic systems with unique functions and collaborative abilities. Miniature robots incorporating insect-like locomotion would have a unique capacity for exploration and action in otherwise inaccessible environments. Meanwhile, mass-produced micro-robots would be suited to economical collaborations of multiple robots, enhancing performance in a variety of robotic applications.

Many researchers have developed legged micro-robotic systems at scales smaller than 20 mm, with varying levels of functionality. The first legged micro-robot capable of autonomous motion was powered by solar cells and

Received June 15, 2007; accepted September 30, 2007.
*Corresponding author. E-mail: kenn.oldham@arl.army.mil

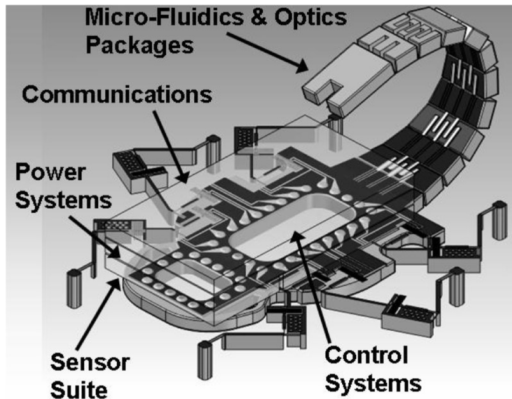

Figure 1. Concept drawing of a bio-inspired micro-robot.

driven by two silicon legs attached to an inch-worm electrostatic motor [1]. Other researchers have relied on thermal actuation techniques, but to date these have relied upon tethered power supplies [2–5], although sufficient weight bearing capability is claimed for battery power; one research group proposes using light focused by micro-lenses for external heating [6]. Another tactic is to use electrostatic scratch drive actuators, which provide low-power, high force actuation, but required power supplied by RF [7] or substrate [8] sources. At slightly larger scales, researchers have examined shape-memory alloys [9], elastomers [10], ion-exchange polymers [11], and piezoelectric ceramics [12].

Unfortunately, the mobility of previous microrobotic systems has been limited, largely due to constraints on actuators available for locomotion. Most of the micro-robots described above utilize single degree-of-freedom legs or cilia in order to support large payloads, which are necessary to supply sufficient power for the actuation methods utilized. This significantly limits the maneuverability of the micro-robots, which typically have step lengths on the order of nanometers to hundreds of micrometers.

An alternative tactic to micro-robotic design is to produce much less massive micro-robots relying upon smaller, lower-power actuators. The reduced mass (for both actuators and power supplies) would permit wide joint angles (10–50 degrees) from multi-degree of freedom legs, resulting in bio-inspired motions, as in the insect/arachnid-like conceptual robot shown in Fig. 1. A typical actuator would be just a few hundred microns in length or width, with several such actuators located at the base of each joint. By sweeping long legs ($\sim$4 mm) through wide joint angles, step lengths of several millimeters could be achieved. However, achieving this mobility from MEMS-type architectures requires very large lateral actuation forces and/or displacements, given the target actuator size. Piezoelectric actuation may provide a very compact, lightweight, and low-power mechanism for operating micro-robotic joints, if piezoelectric

forces can be harnessed to generate in-plane, lateral displacements. PZT lateral micro-actuators have been demonstrated previously [13, 14], but without sufficient force for the micro-robot configuration proposed.

In this paper, the actuation requirements of a bio-inspired terrestrial microrobot are explored in conjunction with the performance of a thin-film piezoelectric microactuator design that can meet these requirements. We begin by discussing fundamental behavior of MEMS flexures as building blocks for microrobotic joints, and implications for actuator design. The potential for piezoelectric thin-films to meet these actuation requirements is examined, along with a brief process description for one method of fabricating the lateral piezoelectric actuators. Experimental results for a set of U.S. Army Research Laboratory (ARL) lateral piezoelectric microactuators are presented, and compared to other common MEMS actuation techniques. Finally, the performance of these components is related briefly to system-level requirements of a functional microrobotic platform.

II. MODELING

a. Flexure Design and Actuator Specifications

Elastic flexures or springs typically provide freedom for motion in MEMS devices. To emulate motion at an insect leg joint, a flexure (or array of flexures) in a micro-robot must bend through an angular range of ten degrees or more. Meanwhile, the flexure must also be capable of supporting a substantial amount of weight. These two requirements place have very different implications for flexure design, and hence for actuator intended to drive bending movement of the flexures.

Consider a scenario in which a series of flexures is used to achieve large rotation angles, the present target angle being forty degrees. Assuming that each of eight individual flexures in the series has a relatively small deflection (five degrees in this scenario), we can model joint rotation due to bending using simple beam theory for a cantilever beam. A schematic view of a single spring/actuator combination is shown in Fig. 2. The maximum angle at the tip of the flexure will be achieved when a uniform bending moment is applied to the flexure, with maximum stress within the flexure equal to the yield stress of the material, or some specified fraction of that stress. The actuation moment, M_{req}, required in this scenario is given by the equation

$$M_{req} = S_{\max}\frac{w^2 t}{6} \tag{1}$$

Here, $S_{\max}$ denotes a maximum bound on axial stress within the flexure, w is the width of the flexure, and t is the thickness of the flexure. The angle in

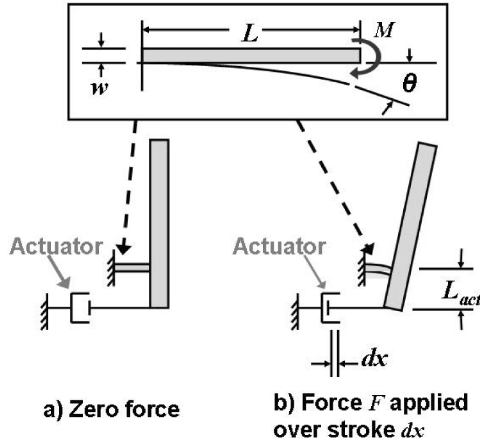

Figure 2. Schematic view of rotational motion using a simple flexural spring (inset).

radians, $\theta_{\max}$, achieved by this flexure will be

$$\theta_{\max} = \frac{2S_{\max}L}{Ew}. \tag{2}$$

In this equation, L is the length of the flexure, while E is the modulus of elasticity of the flexure material.

To calculate the weight bearing capacity of this flexure, consider the stresses and displacements arising in the flexure due to a moment caused by a gravity force, W, acting at the tip of the leg, a distance L_{leg} away. Two potential failure mechanisms are yield or fracture of the flexure, or excessive sag at the flexure. In the first case, the weight limit of the flexure is given by the equation

$$W = \frac{S_{\max}t^2w}{6L_{leg}}. \tag{3}$$

In the second case, setting a maximum sag angle (in radians) θ_{sag}, the weight limit is

$$W = \frac{\theta_{sag}wt^3E}{12LL_{leg}}. \tag{4}$$

The second case is typically more stringent, as in an example in which motion at each joint is monitored by a capacitive sensor, which must be kept closely in plane to function properly. When the second case is used to dictate a weight limit, there is an inverse relationship between maximum tip angle and maximum weight capacity as a function of the ratio of flexure length to width, L/w.

Table 1
Spring design parameters used to estimate micro-robotic actuation requirements

Material	Units	Silicon	Polymer (parylene)
Thickness	μm	10	50
Width	μm	8	4
Length range	μm	10–120	10–90
Elastic modulus	GPa	150	3.2
Maximum stress	MPa	600	50

Now, suppose the actuation moment for each flexure is generated by a MEMS actuator applying an input force, F, parallel to the flexure and offset by a moment arm with length L_{act}. While deforming the flexure, the actuator tip moves through a linear distance dx. The moment applied to the flexure can then be written as $F \cdot L_{act}$, while the maximum angle at the tip of the flexure is approximately dx/L_{act}. This results in a force-displacement product at the microactuator of

$$F \cdot dx = \frac{M_{req}}{L_{act}} \cdot \theta_{\max} L_{act} = \frac{S_{\max}^2 t w L}{3E}. \quad (5)$$

This provides an estimate for the maximum product of force and displacement required by an actuator in a microrobotic system. Note that this is not exactly the same as the maximum work required from the actuator, as the force applied by the actuator is generally not constant over this range of motion. For a flexure that behaves as a linear spring, the maximum work done by the actuator is one-half the maximum product of force and displacement. The latter product is a convenient figure of merit for this application because it corresponds directly to the angle through which an actuator can bend a given flexure.

Figure 3 shows the implications of the above equations for spring design under two flexure fabrication processes, one that produces 10 μm thick flexures built from silicon, and a second that produces 50 μm thick flexures built from a polymer material. A leg length of 4 mm and maximum sag angle of 0.005 radians per flexure were selected based on other system requirements. In the figure, the length of each flexure is varied to show the range of potential bending angles and weight limits. Material properties used in these calculations are given in Table 1.

Figure 3 clearly shows the inverse relationship between weight bearing capability and tip angle. Furthermore, while force-displacement requirements can vary with the flexure selection and flexure width used, an approximate force-displacement product of at least $1 \cdot 10^{-9}$ N $\cdot$ m is required for

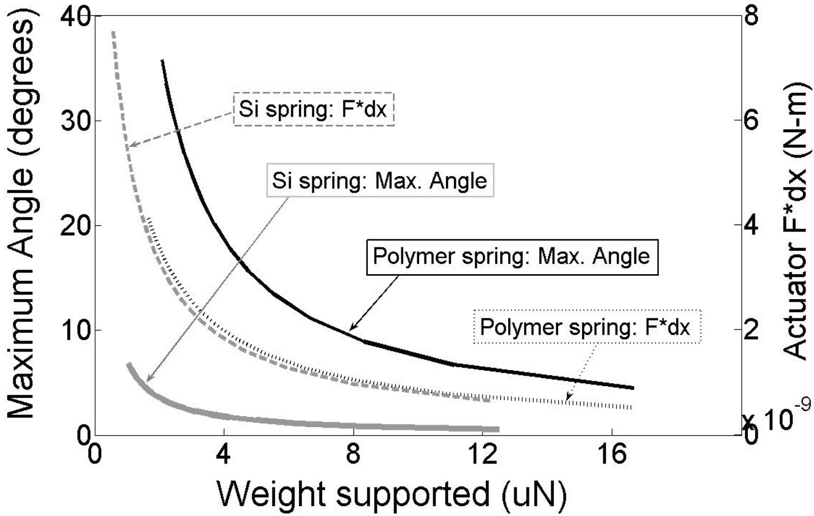

Figure 3. Maximum tip angle (solid lines, left axis) achieved by simple flexural springs as a function of maximum supportable weight, and resulting force times displacement product (dashed lines, right axis) required to reach that maximum angle. Sample silicon and polymer properties are listed in Table 1.

micro-robotic applications using the processes described, which translates to very large forces, displacements, or both from a MEMS-type actuator.

b. Thin-film PZT Capabilities

One actuation technology that has potential for achieving the desired level of performance in a compact area is piezoelectric thin-film actuation. A look at the behavior of a PZT thin-film during axial contraction illustrates this fact. Consider a beam consisting of a thin layer of PZT between two identical platinum electrodes. The magnitude of axial contraction dx of the beam against an external resisting force F is

$$dx = \frac{d_{31}\frac{V}{t_{PZT}}A_{PZT}E_{PZT} - F}{2A_{Pt}E_{PT} + A_{PZT}E_{PZT}}L_0 \tag{6}$$

Here, d_{31} is a piezoelectric strain coefficient, V is the applied voltage, and t_{PZT} is the thickness of the PZT thin-film. E_{PZT} and E_{Pt} are the elastic modulus of PZT and platinum, respectively, and A_{PZT} and A_{Pt} the cross-sectional areas of the PZT and platinum layers of the beam.

Table 2
Thin-film piezoelectric lateral actuator design parameters

Variable	Units	Value
d_{31}	m/V	$130 \cdot 10^{-12}$
t_{PZT}	μm	0.80
w_{PZT}	μm	100
L_0	μm	500
E_{PZT}	GPa	56
E_{Pt}	GPa	170
t_{Pt}	μm	0.05

Inserting the mechanical and piezoelectric properties of thin-film PZT and platinum electrodes (see Table 2) into (6) produces a maximum force-displacement product of approximately $5 \cdot 10^{-9}$ N-m at 20 V in a 500 μm by 100 μm area. Furthermore, this actuation force exceeds that produced by other common MEMS actuation technologies in an equivalent area, while drawing limited power and possessing a relatively small mass compared to other actuation technologies. As a result of such compact, high-force actuation modes, PZT thin-film microactuators have great potential as an enabling technology for bio-inspired micro-robotics.

III. EXPERIMENTAL RESULTS

In practice, it is difficult to create a thin-film piezoelectric actuator that acts in precisely the simple manner described above. Imbalance between electrode layers, residual stresses, nonlinearities in piezoelectric response, and other factors can cause deformation of the piezoelectric beam that differs from the idealized model described above. A separate drawback of simple piezoelectric contraction is limited stroke length; typical piezoelectric films exhibit less than 1% contraction, when many applications require a much larger stroke.

The U.S. Army Research Lab has designed, modeled, fabricated and tested a thin-film PZT lateral actuator that incorporates unique aspects of thin-film behavior into actuator design to extend the maximum displacement of piezoelectric thin films while retaining high forces over shorter stroke lengths. This lateral actuator's force displacement curve as calculated from both an analytical model and experimental test results at 20 V are shown in Fig. 4, along with the force-displacement curve of the idealized actuator described in Section IIb. Due to patent proceedings, full details of actuator design are not currently available for public release; it will simply be noted that further manipulation of the actuator geometry results in a greatly extended tip displacement when resisting force is low, and that these displacements are achieved without the use

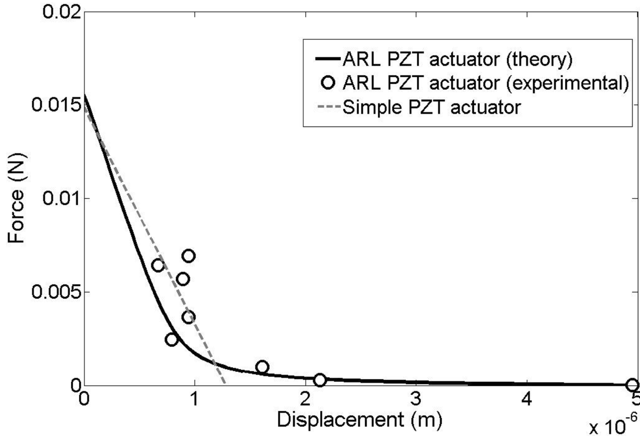

Figure 4. Force-displacement curves for the ARL PZT lateral actuator and simple idealized actuator modeled in Section IIb, compared to experimental actuation measurements.

of mechanical advantage external from the actuator. This paper will concentrate on results in small-displacement motion of the lateral actuator, in which actuator deformation is very similar to idealized contraction.

Thin-film lateral actuators are fabricated on a silicon-on-insulator wafer with a 10 μm thick device layer. The wafer is passivated with a PECVD silicon oxide film and coated with a platinum electrode. Thin-film PZT is deposited to a thickness of 0.8 μm via a sol-gel process, followed by annealing and deposition of a second platinum electrode. Platinum and PZT layers are patterned with a combination of ion-milling and wet etching steps. Silicon structural components are defined by deep reactive-ion etching through the silicon and buried oxide. Actuators are released from the substrate by an isotropic XeF2 etch, with photoresist coating of silicon structures to be preserved through the release process. The actuators tested experimentally differ from the idealized PZT actuator described in Sec.IIb in two details: the presence of a silicon oxide layer beneath the bottom electrode, and proprietary changes to the top electrode to account for the oxide's effects on displacement, serving also to extend actuator stroke length.

Performance of the completed lateral actuators was measured by observing deflection of silicon cantilever beams attached to the tips of test actuators. A sample beam in its released state after application of 20 V to the PZT actuator is shown in Fig. 6. Angular deflections from the free, released position were measured using an optical profilometer, with forces and displacements of the actuator calculated from bending beam theory. The piezoelectric strain coefficient was calculated from out-of-plane deflection of simple PZT cantilevers, again measured using an optical profilometer. Measurement precision

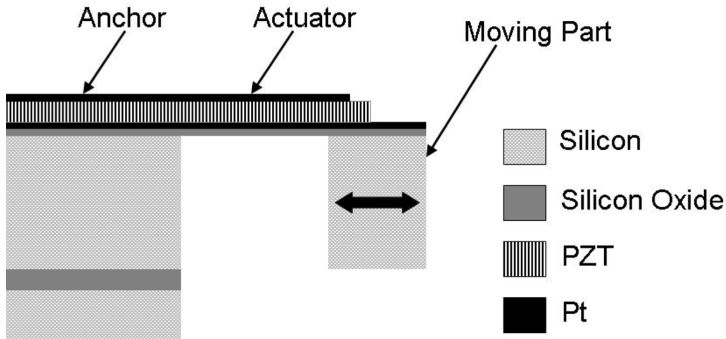

Figure 5. Cross-sectional view of a lateral PZT actuator.

is limited by the resolution of the profilometer, but the trends in experimental force-displacement measurements are consistent with the ARL lateral actuator analytical model.

The nominal power draw of piezoelectric actuators of the size tested due to leakage current at 20 V is approximately 3 nW, based on measurements from capacitive test structures. In addition, the dielectric constant of thin-film PZT capacitors corresponds to just 10 nW of energy required to charge the actuator each time 20 V is applied. The limited power draw of piezoelectric thin films is critically to the ability to eventually support sufficient battery mass from MEMS flexure-based robotic joints.

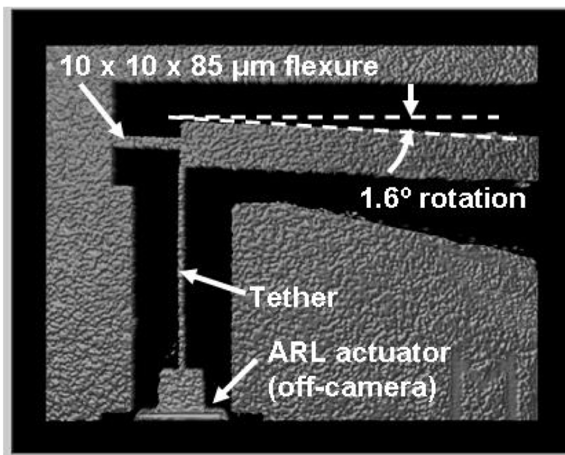

Figure 6. Optical profilometer image showing rotational displacement of a 10 μm thick silicon flexure using an ARL PZT lateral actuator (actuator tip at bottom of image).

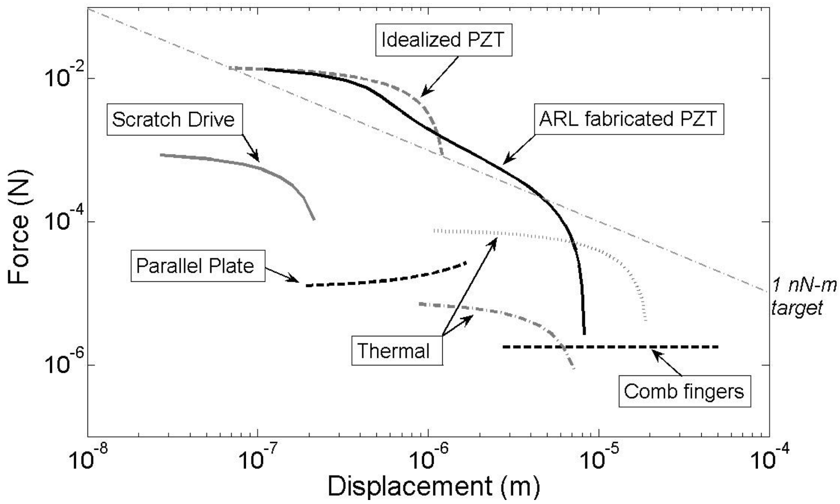

Figure 7. Force-displacement curves for sample MEMS micro-actuators utilizing various actuation mechanisms. The straight line marks the target 1 nN-m minimum performance for micro-robotic applications. 50000 μm^2 actuators at 20 V.

Figure 7 shows the analytical force displacement curve of the simple PZT actuator hypothesized above in comparison with the force displacement curves of several other MEMS lateral micro-actuators. This comparison of specific actuators of various types provides a reference point for evaluating PZT lateral actuator results. In all cases, the total actuator area is 50000 μm^2; when individual actuators require less space, an array of actuators is considered. All curves are drawn for input voltages of 20 V, with the exception of the scratch drive array, acting at 60 V.

Force-displacement curves for electrostatic actuators are taken from equations

$$F_{cf}(x) = \frac{1}{2}\varepsilon_0 \frac{t}{g_0} N_f V^2 \tag{7}$$

$$F_{pp}(x) = \frac{1}{2}\varepsilon_0 \frac{t L_f}{(g_0 - x)} N_f V^2 \tag{8}$$

for comb-finger (F_{cf}) and parallel plate (F_{pp}) respectively. Here, ε_0 is the permittivity of air, t is the device thickness, L_f is the actuator finger length, N_f is the number of fingers, g_0 is the nominal gap between fingers, and V is the driving voltage. For this example, both actuator types consist of 5 μm gap and finger widths in a 100 μm thick device, a moderately aggressive aspect ratio. The number of fingers is selected to fill the 50000 μm^2 total area of the other actuators, with a 50 μm stroke length selected for the comb finger actuator.

Thermal actuator and scratch drive curves are estimated using linear interpolation and extrapolation from experimental data points published in references [15], [16], and [7]. It should be noted that this technique may understate performance of thermal actuators; the chief disadvantage of small thermal actuators for micro-robotic applications is power consumption, rather than force generation. When individual actuators are smaller than the actuation area of comparison, additional actuators are added in parallel to fill the allotted space, resulting in an array of 6 scratch drive elements and 20 thermal actuation elements of the type described in [7]. Electromagnetic actuation (not shown) may also be capable of reaching the $1 \cdot 10^{-9}$ N $\cdot$ m target, but again requiring high power consumption.

As is apparent in Fig. 7, if a simple thin-film PZT actuator were realized in the manner described above, it would feature a maximum force much larger than that of other common actuator technologies, while retaining reasonable levels of displacement. The experimentally verified ARL lateral actuator is slightly reduced in force, but also meets micro-robotic specifications. Furthermore, piezoelectric technology may be the only actuation technique capable of meeting the micro-robotic force-displacement requirements specified, in the spatial area described and with low power consumption.

IV. CONCLUSION

Compact, high-force, low-power thin-film piezoelectric actuators could serve as an enabling technology for bio-inspired micro-robotics. The United States Army Research Laboratory has demonstrated thin-film PZT lateral actuators with large forces ($\sim$8 mN) over strokes of almost 1 μm in a 500 μm by 100 μm footprint. These actuation forces exceed those of other common MEMS actuation techniques acting with similar footprints and voltages, and furthermore can meet actuation specifications for insect-like micro-robotic joints. ARL PZT lateral actuators will be incorporated with high-aspect ratio silicon or polymer microstructures to produce micro-robotic platforms with capacities for innovative maneuverability and locomotion.

REFERENCES

1. S. Hollar, A. Flynn, C. Bellow, and K. S. J. Pister, Solar powered 10 mg silicon robot. MEMS Kyoto. Japan 706–711 (2003).
2. P. E. Kladitis and V. M. Bright, “Prototype microrobots for micro-positioning and micro-unmanned vehicles.” *Sensors and Actuators A: Physical* **80**, 132–137 (2000).
3. A. Bonvilain and N. Chaillet, “Microfabricated thermally actuated micro-robots.” *Proc. 2003 IEEE Intl. Conf. Robotics Automation. Taipei, Taiwan* 2960–2965 (2003).

4. T. M. Ebefors, U. Johan, E. Kälvesten, and G. Stemme, “A walking silicon micro-robot,” *Proc. 10th Intl. Conf. Solid-State Sensors Actuators* Sendai, Japan 1202–1205 (1999).
5. M. H. Mohhebi, M. L. Terry, K. F. Böhringer, G. T. A. Kovacs, and J. W. Suh, “Omnidirectional walking microrobot realized by thermal microactuator arrays,” *Proc. ASME Intl Mech. Eng. Congress* New York, NY, USA 1–7 (2001).
6. S. Baglio, S. Castorina, L. Fortuna, and N. Savalli, “Development of autonomous, mobile micro-electromechanical devices,” *Circuits and Systems Phoenix* AZ, USA 285–288 (2002).
7. P. Basset, A. Kaiser, P. Bigotte, D. Collard, and L. Buchaillot, “A large stepwise motion electrostatic actuator for a wireless microrobot,” *MEMS Las Vegas* NV, USA 606–609 (2002).
8. B. R. Donald, C. G. Levey, C. D. McGray, I. Paprotny, and D. Rus, “An untethered, electrostatic,” globally controllable MEMS micro-robot. *JMEMS.* **15**(1), 1–15 (2006).
9. Y. P. Lee, B. Kim, M. G. Lee, and J.-O. Park, “Locomotive mechanism and fabrication of biomimetic micro robot using shape memory alloy,” *Proc. IEEE Conf. on Robotics and Automation* New Orleans, LA, USA 5007–5011 (2004).
10. H. R. Choi, S. M. Ryew, K. M. Jung, H. M. Kim, J. W. Jeon, J. D. Nam, R. Maeda, and K, Tanie, “Micro robot actuated by soft actuators based on dielectric elastomer,” *Proc. IEEE/RSJ Conf. on Intelligent Robots and Systems. Lausanne, Switzerland: IEEE* 1730–1735 (2002).
11. B. K. Kim, J. W. Ryu, Y. K. Jeong, Y. H. Tak, B. M. Kim, and J.-O. Park, “A ciliary based 8-legged walking micro robot using cast IPMC actuators,” *Proc. IEEE Intl. Conf. on Robotics and Automation* Taipei, Taiwan IEEE 2940–2945 (2003).
12. U. Simu, and S. Johansson, “Analysis of quasi-static and dynamic motion mechanisms for piezoelectric miniature robots,” *Sensors and Actuators A: Physical* **132**(2), 632–642 (2006).
13. Y. H. Seo, D.-S. Choi, J.-H. Lee, T.-M. Lee, T.-J. Je, K.-H. Whang, “Piezoelectric actuator based on stiffness control and stroke amplification for large lateral actuation.” *MEMS* Miami, FL USA 383–386 (2005).
14. N. J. Conway, Z. J. Traina, and S.-G. Kim, “A strain amplifying piezoelectric actuator.” *J. Micromech. Microeng* **17**, 781–787 (2007).
15. M. J. Sinclair, “A high force low area MEMS thermal actuator.” *7th Intersoc. Conf. Thermal Thermomechanical Phenomena.* Las Vegas NV, USA 129–132 (2002).
16. C. S. Pan, C.-L. Chang, and Y.-K. Chen, “Design and fabrication of an electro-thermal microactuator with multidirectional in-plane motion.” *J Microlith., Microfab., Microsyst* **4**(3), 1–15 (2005).